

IIII The Kikuchi-Kossel Experiment - Colloidal Crystals under Microgravity IIII
(Original Paper)

Structural Characterizations of Charged Colloidal Crystals

Chiho KAKIHARA¹, Akiko TOYOTAMA¹, Tohru OKUZONO¹, Junpei YAMANAKA¹,
Kensaku ITO², Tadatomi SHINOHARA³, Masayuki TANIGAWA³ and Ikuo SOGAMI³

Abstract

We examined influences of the particle volume fraction ϕ and effective charge number Z_{eff} on the crystal structures of charged colloids, by means of the reflection spectroscopy and Kikuchi-Kossel diffraction measurements. We employed dilute salt-free aqueous dispersions of charged polystyrene (PS) particles (the diameter $d = 110$ to 120 nm; $Z_{\text{eff}} =$ about 1300) and colloidal silica ($d = 120$ nm, $Z_{\text{eff}} =$ about 550). The PS colloids had the BCC structure at $\phi \leq 0.01$ and exhibited the structural phase transition into the FCC lattice on increasing ϕ . The silica colloids, which had lower Z_{eff} , took the BCC structures at all ϕ s examined ($\phi \leq 0.04$).

Keyword(s): charged colloidal crystal, BCC-FCC phase transition, reflection spectroscopy.

Received 31 Dec. 2014, accepted 10 Mar. 2015, published 31 Apr. 2015

1. Introduction

Submicron-sized charged colloidal particles dispersed in liquid medium self-assemble into ordered “crystal” structures¹⁻⁵. In the crystal states, the particles are regularly arranged in the body-centered-cubic (BCC) or face-centered-cubic (FCC) lattices.

We have prepared colloid samples for microgravity experiment project on the colloidal crystallization in the international space station (“Structure analysis of colloidal crystals under the microgravity environment by laser diffraction and investigation of colloidal interaction”); principal investigator, Ikuo Sogami⁶). This project aims at precise structural characterizations of the colloidal crystals under microgravity, by applying the Kikuchi-Kossel diffraction measurements. We are planning several themes as the space experiments. Precise determinations of the crystal structures and examinations of influences of major parameters, *e.g.*, particle volume fraction ϕ and charge number Z to the crystal structures will be one of the topics in the space experiments.

In the present paper, we report the structural characterizations of the colloidal crystals of charged polystyrene (PS) and colloidal silica dispersions, which have been prepared for the space experiments. The crystal structures were determined by reflection spectroscopy, and also by Kikuchi-Kossel diffraction experiments. We will demonstrate that the FCC structures were formed when the ϕ and/or Z values were high, while the BCC crystals were observed at low ϕ and Z . The present results will be useful to set the conditions in the space experiments.

2. Experimental Section

2.1 Materials

The PS particles were synthesized by an emulsifier free polymerization method⁷. Styrene monomer (Wako Co., Ltd.) was mixed with an aqueous solution sodium hydroxide (NaOH) and shaken to extract coexisting polymerization inhibitors into the aqueous phase. Divinyl benzene (DVB, crosslinker, Nacalai Co., Ltd.) was washed by aqueous NaOH solution by a similar manner. Water (210 mL), methanol, styrene (20 mL), DVB (1 mL), and an anionic co-monomer sodium *p*-styrenesulfonate (NaSS, Wako) were introduced into a 300 mL separable flask, equipped with a reflux condenser. The reaction mixture was stirred at 600 rpm by using a magnet stirrer, at 80 °C for 30 min, under an argon atmosphere. Then, a radical polymerization initiator, potassium persulphate (0.1 g, Kanto Chemical Co., Ltd.) was added to the reaction solution, and the solution was further stirred. A turbid dispersion of charged polystyrene particles was obtained after 7 h. Twelve kinds of samples were synthesized at various methanol and NaSS concentrations. The compositions of the reactions solutions will be shown in Table A1 of Appendix.

An aqueous dispersion of colloidal silica, KE-P10W was purchased from Japan Catalyst Co., Ltd. (Osaka).

All these colloid samples were purified by dialysis against purified water for about a month. Then, a mixed bed of anion- and cation- exchange resin beads, AG-501-X8D (Bio-Rad Labs, CA, U.S.A) was added to the samples, and they were kept standing for further deionization at least for a week.

1. Faculty of Pharmaceutical Sciences, Nagoya City University, 3-1 Tanabe, Mizuho-ku, Nagoya City 467-8603, Japan.
2. Faculty of Engineering, Toyama University, Gofuku, Toyama City 930-8555, Japan.
3. Faculty of Science, Kyoto Sangyo University, Motoyama, Kamigamo, Kita-ku, Kyoto City, 603-8555, Japan.
(E-mail: yamanaka@phar.nagoya-cu.ac.jp)

The PS particles had negative surface charges resulted from sulfonic acid groups ($-\text{SO}_3^- \text{H}^+$) on the copolymerized NaSS, and the sulfuric acid groups ($-\text{SO}_4^- \text{H}^+$) arising from KPS. After the purifications, the counterions of these charged groups were converted to H^+ ions. The silica particles were slightly charged due to dissociations of silanol groups ($\text{Si-OH} \leftrightarrow \text{Si-O}^- + \text{H}^+$) on their surfaces, which are weak acids.⁸⁾ The dissociation degree of the silanols, and thus the Z value of silica particles, was controlled by additions of $80 \mu\text{M}$ NaOH⁹⁻¹¹⁾.

The characteristics of the colloidal particles used are compiled in **Table 1**. Here, d is the particle diameter determined by dynamic light scattering method, and Z_{eff} is the effective charge number; Z_{eff} of the PS particles were determined by the electrical conductivity measurements¹¹⁾, while for the silica particles, Z_{eff} was estimated based on the relationship between Z_{eff} and NaOH concentrations (c , in μM) determined in our previous study¹²⁾,

$$Z_{\text{eff}} = 207.43 + 4.9045c - 0.0084434c^2.$$

All the samples used for the crystallization experiments were prepared by diluting stock dispersions with Milli-Q water. We prepared the samples without additions of extraneous salts.

2. 2. Methods

Reflection spectra of the crystals were measured by using fiber optics spectrophotometers, type USB2000, Ocean Optics Co., Ltd (FL, U.S.A.). 1mL of the samples were introduced into the poly(methylmethacrylate) cell having an inner dimension of $1 \times 1 \times 4.5$ cm. The spectra of the samples were measured 1 h after homogenizing the sample by shaking.

Laser diffraction measurements were performed by means of Kossel diffraction apparatus constructed in Kyoto Sangyo University, whose details have been reported elsewhere¹³⁾. Quartz cuvettes ($0.1 \times 1 \times 4.5$ cm) were used as sample cells. A He-Ne laser (wavelength = 633 nm) was used as a light source. The forward diffractions from the crystals were recorded by using a CCD camera.

3. Results and Discussion

3.1 Structural characterization by spectroscopy

The crystal structures were examined by means of reflection spectroscopy. Diffraction wavelength λ_B of colloidal crystals are represented by the Bragg relation $2d_{hkl}\sin\theta = n\lambda_B/n_r$, where d_{hkl} is a spacing between (h, k, l) crystal planes, θ the incident angle of light, n an integer, and n_r the refractive index of the crystals. Under dilute conditions, n_r can be approximated in terms of a volume averaged value, $n_r = (1-\phi)n_{r,m} + \phi n_{r,p}$, where $n_{r,m}$ and $n_{r,p}$ are refractive indexes of the medium (water, =1.33) and particles (PS, 1.60; silica, 1.45), respectively. For the BCC lattices, the diffractions arises from (110), (200), (211)... planes, while (111), (200), (220)... lattice planes provide the diffraction of the FCC structures¹⁴⁾. In **Fig. 1**, lattice structures and several lattice planes are illustrated. For the cubic lattices, $d_{hkl} = a/(h^2 +$

Table 1 Characteristics of particles.

Sample	composition	d (nm)	Z_{eff}
KSS-05	PS ^a	119 ± 12	1290
KSS-06	PS	109 ± 12	1180
KSS-08	PS	117 ± 11	1290
KE-W10 ^b	silica	120 ± 11	550

a: polystyrene

b: NaOH concentration = $80 \mu\text{M}$

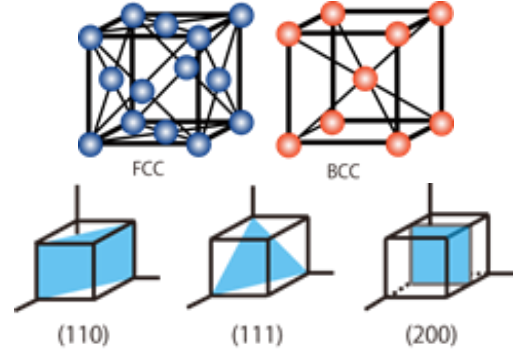


Fig. 1 Illustrations of the FCC and BCC crystal lattices and the lattice planes.

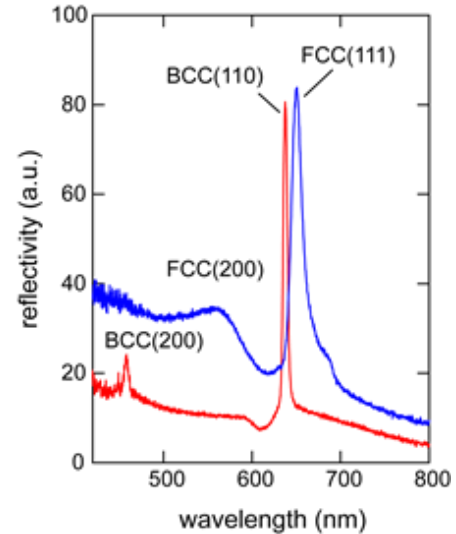


Fig. 2 Reflection spectra of the colloidal crystals of the silica ($\phi = 0.03$, a red curve) and PS (KSS-06, $\phi = 0.025$, a blue curve) dispersions.

$k^2 + l^2)^{1/2}$, where a is the lattice constant. This implies that the λ_B values of the first order ($n = 1$) diffractions from the BCC lattice planes should have a ratio $1: 1/\sqrt{2}: 1/\sqrt{3} \dots$. On the other hand, for the FCC lattices, the ratio of λ_B values is $1/\sqrt{3}: 1/2: 1/2\sqrt{2} \dots$. Thus, we can determine the crystal structures by the spectroscopy.

In **Fig. 2**, the reflection spectrum of the colloidal silica ($\phi = 0.03$) is shown by a red curve. Two distinct peaks were observed at $\lambda_B =$ about 640 nm and 460 nm, which were attributable to the diffractions from the BCC lattice. On the other hand, the

spectrum of PS colloids (KSS-06, $\phi = 0.025$). The blue curve in **Fig. 2**, $\lambda_B = 650$ nm and 575 nm), was attributed to the FCC structures.

We note that a small peak corresponding to the second diffraction of the BCC lattices was frequently observed for the PS crystals, usually in 5 min after the homogenization, which disappeared over time. This suggests that the FCC/BCC coexistence structures were formed initially, although the equilibrium states of these samples were the FCC crystals¹⁵. The detailed study on the time evolution and dynamics of the crystal structure is in progress.

3.2 Influence of the particle concentration

Figure 3 shows λ_B values for PS (KSS-06) colloids at various values of ϕ . The blue and red colored circles in **Fig. 3** are the λ_B s for the observed first and second diffractions, respectively. The solid and dashed curves represent λ_B values for the FCC and BCC crystal lattices calculated from the ϕ values: for homogeneous crystals, λ_B of the diffraction from the BCC (110) is given by

$$\lambda_B = \sqrt{2} n_r (8\pi/3 \phi)^{1/3} a_p$$

while for FCC (111) planes

$$\lambda_B = (2/\sqrt{3}) n_r (16\pi/3 \phi)^{1/3} a_p$$

respectively, where a_p is the particle radius. When the a_p value determined by the dynamic light scattering was used, the calculated λ_B values were larger than the observed ones by about 14%. This might be caused by inhomogeneity in the colloids, although influences of sedimentation cannot be ruled out. We note that effect of the sedimentation against Brownian motion of the particles is represented by Péclet number $Pe =$

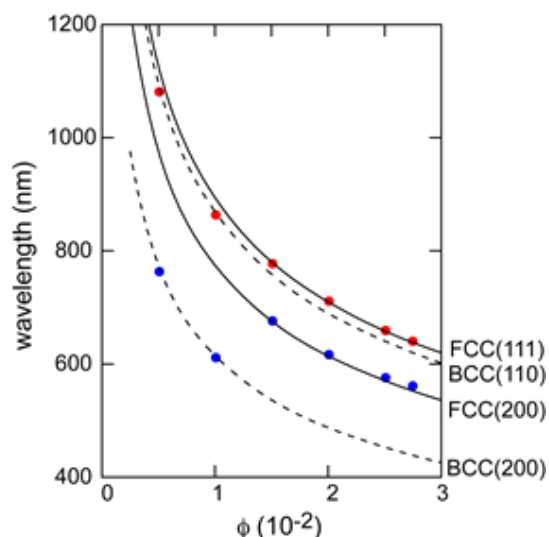


Fig. 3 Bragg wavelengths λ_B for colloidal crystals at various values of ϕ . Sample, the KSS-08 PS dispersions. The red and blue symbols are the observed first and second diffractions; the solid and dashed curves are calculated values of λ_B for the FCC and BCC crystal lattices.

$4\pi a_p^3 \Delta\rho g h / 3k_B T$.²⁾ Here $\Delta\rho$ is the density difference between the particle and medium, g is the gravitational acceleration, and $k_B T$ is the Boltzmann temperature. An effect of gravitational sedimentation on the phase behavior of colloids has been studied by Masri et al.¹⁶⁾, based on microscopic Péclet number ($h \sim a_p$). The values of macroscopic Pe for our PS/water and silica/water systems ($h = 1$ cm) were about 10 and 110, respectively, which implies that the effect of sedimentation is not negligible at least in the absence of the electrostatic interaction. Microgravity experiments will be helpful to elucidate the observed discrepancy.¹⁷⁾

Here, we fitted the experimental values by varying a_p . The curves shown in **Fig. 3** were drawn by assuming $a_p = 48$ nm, which showed close agreements with the experiments. With increasing ϕ , the crystal structures changed from the BCC to FCC structure at $\phi = 0.01 \sim 0.015$. The BCC to FCC structural transition was also observed for KSS-05 colloids at $\phi = 0.01 \sim 0.015$. On the other hand, the silica crystals showed the BCC structures at $\phi \leq 0.04$. Because the size and size-polydispersity of the PS and silica samples were not significantly different from each other, the observed difference in the lattice structures appears to be due to the higher Z of the PS than that of silica.

3.3 Kikuchi-Kossel diffraction measurements

In the space experiment project, Kikuchi-Kossel diffraction apparatus (CCOF) has been constructed to determine the crystal structure precisely¹⁸⁾. Here we measured the diffraction by using the apparatus that has been developed in Kyoto Sangyo University. **Figure 4a** and **4b** is the diffraction patterns for the PS (KSS-06, $\phi = 0.03$) and silica ($\phi = 0.04$) colloidal crystals. When the close-packed lattice planes [(111) and (110) planes for FCC and BCC planes, respectively] are oriented parallel to the container wall and the direction of the incident laser beam is normal to the container wall, the diffraction pattern from the BCC and FCC structures have two-fold and three-fold symmetric pattern. As seen in **Fig. 4a**, the diffraction from the PS colloids are attributed overlapped, two antiparallel three-fold-symmetric diffractions. This indicates that twin FCC structures are formed. On the other hand, the diffraction from the silica crystals had two-fold symmetry, implying that the crystals had BCC structures. Laser diffraction patterns from various other colloidal crystals are reported in the reference 19.

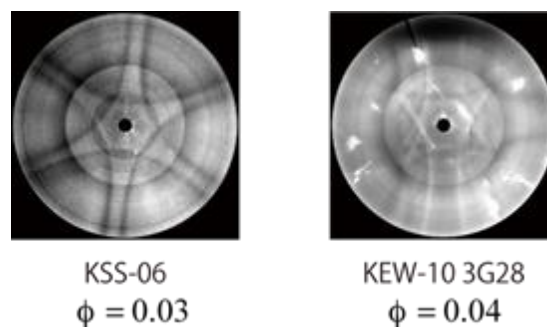


Fig. 4 Kossel diffraction patterns for the colloidal crystals of PS (KSS-06, $\phi = 0.03$; left) and silica ($\phi = 0.04$; right).

We note that the diffraction of the KSS-08 crystals ($\phi = 0.03$) also attributed to the FCC structure. These observations agreed with the results by the spectroscopy.

In previous studies on the charged colloidal crystals²⁻⁵, the BCC and FCC structures were observed at low and high particles concentrations, respectively, which was explainable to a difference in the concentration dependence of the free energies of the BCC and FCC structures. The present experimental results showed a good correspondence to these previous works. The influence of Z on the crystal structures has not frequently found in the literature. Because the interaction magnitude is larger at higher values of Z , as well as at higher ϕ , it appears to be reasonable that the FCC is observed at higher Z .

4. Conclusions

We examined the crystal structures of charged colloids by applying the reflection spectroscopy and Kikuchi-Kossel diffraction experiments. The BCC to FCC phase transition occurred in PS colloids upon increasing ϕ . The colloidal silica, which had a lower Z than PS colloids, the crystal structure was attributed to the BCC lattices. We expect that microgravity experiments will provide an ideal tool to elucidate the mechanism of the observed phase behavior.

Acknowledgments

This paper is supported by the 2014 JAXA/ISAS WG fund “Studies Using Model Colloidal Aggregation and Crystallization under Controlled Gravity Field”.

References and Notes

- 1) P. Pieranski: *Contemp. Phys.*, **24** (1983) 25.
- 2) W.B.Russel, D.A.Saville and W.R.Schwalter: *Colloidal Dispersions*, Cambridge University Press, New York, 1989.
- 3) A.Arora and B.V.R.Tata eds.: *Ordering and Phase Transitions in Charged Colloids*, VCH inc., NY, 1996.
- 4) N.Ise and I.Sogami: *Structure Formation in Solution*, Springer, Berlin, 2005.
- 5) A.K. Sood, *Solid State Physics*, H.Ehrenreich and D.Turnbull eds.: Academic Press, New York, 1991.
- 6) I.S. Sogami, T. Shinohara, M. Tanigawa, K. Ito and J. yamanaka: *Int. J. Microgravity Sci. Appl.*, **32** (2015) 320202, JAXA website, <http://iss.jaxa.jp/kiboexp/field/scientific/> (in Japanese).
- 7) T. Grimaud and K.Matyjaszewski: *Macromolecules*, **30** (1997) 2216.
- 8) R.K. Iler: *The Chemistry of Silica*, John Wiley and Sons., New York, 1979.
- 9) J.Yamanaka, T.Koga, N.Ise and T.Hashimoto: *Phys. Rev.*, E **53** (1996) R4317.
- 10) J.Yamanaka, H.Yoshida, T.Koga, N.Ise and T.Hashimoto: *Phys. Rev. Lett.*, **80** (1998) 5806.
- 11) H.Yoshida, J.Yamanaka, T. Koga, N.Ise and T.Hashimoto: *Langmuir*, **15** (1999) 2684.
- 12) A.Toyotama and J.Yamanaka: *Langmuir*, **27** (2011) 1569.
- 13) T.Shinohara, H.Yamada, I.Sogami, N.Ise and T.Yoshiyama: *Langmuir*, **20** (2004) 5141.
- 14) C.Kittel: *Introduction to Solid State Physics*, Sixth Edition, Wiley and Sons, New York, 1993.
- 15) The small shoulder in the spectra of the PS (at 680 nm) and silica (590 nm) were not attributable to any diffraction from FCC and BCC structures; they would be artifact peaks on subtracting background spectra.
- 16) D. E. Masri et al.: *Soft Matter*, **8** (2012) 6979.
- 17) We note that the abovementioned discrepancy would be partly due to experimental errors in determining λ_B . An error in λ_B is equal to $(1/3)\Delta\phi + \Delta a_p$, where $\Delta\phi$ and Δa_p are errors in determining ϕ and a_p , respectively. Thus Δa_p (a few %) is more significantly affect the accuracy in λ_B .
- 18) Y. Ito, H. Tamaru, Y. Nakamura, S. Adachi, T. OKA, T. Tomobe, T. Naide and H. haba: *Int. J. Microgravity Sci. Appl.*, **32** (2015) 320203.
- 19) M. Tanigawa, T. Shinohara, J. yamanaka, K. Ito and I.S. Sogami: *Int. J. Microgravity Sci. Appl.*, **32** (2015) 320204.

Appendix

Table A1 shows influences of the amounts of methanol and NaSS on the particle diameter by the emulsifier free polymerization method. Contents of water (210 mL), styrene (20 mL), DVB (1 mL), KPS (0.1 g) in the reaction solutions were the same for all the samples. By varying the amounts of methanol and/or NaSS, the particle size could be controlled. At larger amounts of methanol, the particle size was larger, as reported by Grimaud et al.⁷⁾ They explained this by (1) a higher solvability of styrene monomer to media (water/methanol mixtures), which increases the critical size of styrene droplets, and (2) reduction of charged species (NaPSS and KPS) per unit volume of medium, by which the stability of the droplets are reduced. The particle size was smaller at higher NaSS concentrations, which was attributable to charge stabilization of the droplets by the NaSS.

Table A1 A relationship between compositions of the reaction solution and the diameter of PS particles.

Sample number	methanol (mL)	NaSS (g)	d (nm)	SD ^a (%)
KSS-01	5	0.8	59	35
-02	5	0.4	85	12
-03	5	0.4	76	25
-04	5	0.2	119	27
-05	5	0.15	118	10
-06	5	0.1	109	11
-07	5	0.05	155	15
-08	5	0.2	111	10
-09	20	0.4	94	8
-10	100	0.4	204	11
-11	20	0.3	113	10
-12	40	0.4	126	15

a: particle size distribution in standard deviation